Photochemistry and Photobiology, 1998, 68(3): 427–431

Rapid Communication

Development of a Fiber Optic Probe to Measure NIR Raman Spectra of Cervical Tissue *In Vivo*

Anita Mahadevan-Jansen*†[1,2], Michele Follen Mitchell[3], Nirmala Ramanujam†[1,4], Urs Utzinger[1], and Rebecca Richards-Kortum[1]

[1]Biomedical Engineering Program, University of Texas, Austin, TX, USA;
[2]Department of Biomedical Engineering, Vanderbilt University, Nashville, TN, USA;
[3]Department of Gynecology, UT MD Anderson Cancer Center, Houston, TX, USA and
[4]Department of Biophysics and Biochemistry, University of Pennsylvania, Philadelphia, PA, USA

Received 7 July 1998; accepted 22 July 1998

ABSTRACT

The goal of this study was to develop a compact fiber optic probe to measure near infrared Raman spectra of human cervical tissue *in vivo* for the clinical diagnosis of cervical precancers. A Raman spectrometer and fiber optic probe were designed, constructed and tested. The probe was first tested using standards with known Raman spectra, and then the probe was used to acquire Raman spectra from normal and precancerous cervical tissue *in vivo*. Raman spectra of cervical tissue could be acquired *in vivo* in 90 s using incident powers comparable to the threshold limit values for laser exposure of the skin. Although some silica signal obscured tissue Raman bands below 900 cm^{-1}, Raman features from cervical tissue could clearly be discerned with an acceptable signal-to-noise ratio above 900 cm^{-1}. The success of the Raman probe described here indicates that near infrared Raman spectra can be measured *in vivo* from cervical tissues. Increasing the power of the excitation source could reduce the integration time to below 20 s.

INTRODUCTION

Several groups have shown the potential of vibrational spectroscopy for cancer diagnosis in various organ sites (1–8). Features of the vibrational spectrum can be related to molecular and structural changes associated with neoplastic transformation. Raman spectroscopy has been investigated for detection of cancers of the breast, brain, colon, bladder, uterus, ovary and cervix *in vitro* (1,2,5,7–10). We have demonstrated the potential of near infrared (NIR)‡ Raman spectroscopy for the differential diagnosis of cervical precancers (9,10). In an *in vitro* pilot study, NIR Raman spectroscopy enabled consistent discrimination of precancerous cervical lesions from samples with inflammation and metaplasia and normal tissues using empirical intensities as well as multivariate statistical algorithms with a sensitivity and specificity of 82% and 92% or better (10). Based on the success of these *in vitro* Raman studies for precancerous cervical tissue recognition, we developed and tested a system to measure cervical tissue Raman spectra *in vivo*.

Because Raman signals are relatively weak in comparison with fluorescence, and many materials used in fiber optic probes are Raman active, an *in vivo* Raman system must be designed to be sensitive and yet have sufficiently low intrinsic signal to permit tissue measurements in a clinical setting. The development of charge-coupled device (CCD) cameras and diode lasers has made it possible to build portable NIR Raman systems with short integration times (9). However, the development of fiber optic probes for remote delivery and collection of Raman spectra *in vivo* has proven to be more challenging. Typically, the optical elements and optical fibers used for light delivery in a remote sensing spectroscopic system are made of silica. Silica has an intense fluorescence and Raman signal that can interfere with the detection of the weak tissue signal (11). The intrinsic spectroscopic signals generated in both the delivery and collection fibers can interfere with the measurement of tissue Raman spectra. A feasible probe design for a clinical system must prevent this unwanted silica signal from being detected as well as allow maximal collection of the weak tissue Raman signal.

In an attempt to circumvent signal interference due to sil-

*To whom correspondence should be addressed at: Department of Biomedical Engineering, Box 1631, Station B, Nashville, TN 37235, USA. Fax: 615-343-7919; e-mail: anitha@vuse.vanderbilt.edu

†When this work was done, Anita Mahadevan-Jansen and Nirmala Ramanujam were with the University of Texas at Austin, Biomedical Engineering Program; Anita Mahadevan-Jansen is now with Vanderbilt University, and Nirmala Ramanujam is now with the University of Pennsylvania, Department of Biophysics and Biochemistry, Philadelphia, PA, USA.

‡*Abbreviations:* ACGIH, American Conference of Governmental Industrial Hygienists, Inc.; CCD, charge-coupled device; CPC, compound parabolic concentrator; NA, numerical aperture; NIR, near infrared; OD, optical density; QE, quantum efficiency; S/N, signal-to-noise ratio; TLV, threshold limit value.

ica, several different types of optical fibers such as sapphire and liquid guide fibers were tested for use in a Raman probe and silica–silica fibers were identified to be the preferred candidate (12). Several different designs of fiber optic probes have been proposed for potential clinical acquisition of Raman spectra (1,3). In a breast tissue study, McCreery *et al.* used two different fiber optic bundles: a 6 × 1 fiber bundle accessible through a biopsy needle and an integrated 2 × 2 inch non-contact probe (DLT, Laramie, WY). These were tested on breast tissue models and breast tissues *in vitro* (1). Fiber interference was found to be more significant in the weaker Raman spectra of cancer samples than normal tissues. Feld *et al.* used a compound parabolic concentrator (CPC) at the distal tip of a probe with multiple collection fibers to yield seven times more signal as compared to using a fiber probe without the CPC to acquire Raman spectra for transcutaneous blood glucose measurements (3). Fiber background was reduced using a dichroic mirror and separate excitation and collection geometries. Puppels *et al.* proposed the use of a "gaser" based probe with filter-coated fibers for application in the esophagus (4). Other successful *in vivo* measurements have been in the eye (5) and skin (6). Published reports of *in vivo* Raman applications have been confined to exposed tissue areas where fiber background could be circumvented using a macroscopic arrangement. However, other organ sites, such as the colon, cervix and oral cavity, require a more compact configuration and probe design.

Thus, the goal of this project was to develop a compact fiber optic Raman probe to acquire Raman spectra of the cervix *in vivo* without significant interference from fiber signal. Toward this goal, a Raman probe was developed; system accuracy was tested using known standards. Finally, cervical tissue Raman spectra were acquired from human patients *in vivo.*

Materials and Methods

System development

Throughput optimization. The *in vitro* system used to measure cervical Raman spectra (described in Mahadevan-Jansen *et al.* (10)) used a macroscopic system consisting of three 1″ diameter quartz lenses and two 1″ diameter filters in the excitation and collection legs. This *in vitro* system required 15 min of integration to yield Raman spectra from cervical tissue biopsies with acceptable signal-to-noise ratios (S/N). This is impractical for *in vivo* cervical studies that require a compact fiber optic probe for remote sensing and a maximum integration time of 2–3 min. An analysis of the throughput of the *in vitro* delivery and collection systems was performed (13) to identify all sources of loss in the optical system. The largest sources of loss of signal were due to the mismatch in the numerical aperture (NA) and spot size at the entrance of the spectrograph and the low quantum efficiency (QE) of the CCD in the NIR spectral region. Based on these results, the fiber optic Raman system was redesigned to increase throughput; Fig. 1 (insert) shows the block diagram of the system designed for improved throughput. It consists of a diode laser at 789 nm, an imaging spectrograph and a CCD camera. To account for the NA mismatch, a fast spectrograph was selected (Holospec f/2.2, Kaiser Optical Systems, Ann Arbor, MI) with an NA of 0.27 comparable to that of a typical optical fiber. Coupling optics in the spectrograph provided 1:1 imaging with minimal optical losses due to NA matching between the spectrograph and fibers. A back-illuminated, deep depletion CCD chip with enhanced QE and reduced etaloning in the NIR (QE ≃ 70% at 900 nm) (Princeton Instruments, Edison, NJ) was used to further reduce integration time.

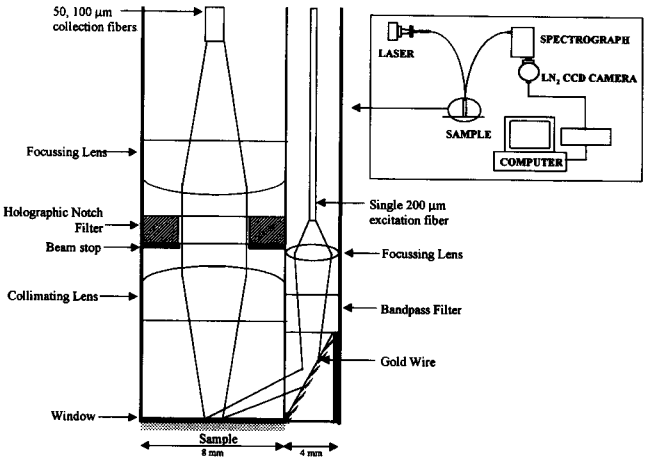

Figure 1. Schematic (transverse section) of the probe used for clinical Raman measurements (not to scale) with an insert of the system block diagram.

Fiber probe development. The diameter and NA of the optical fibers used in the delivery and collection legs of the probe were chosen to maximize the system throughput and collection efficiency. All optical fibers used were 0.22 NA, UV grade silica (quartz) core fibers (Superguide G, thermocoat fibers from Fiberguide Industries, Stirling, NJ). The output of the diode laser has a focused spot size of approximately 200 μm; thus, a single excitation fiber with a 200 μm core diameter was used. The desired spectral resolution of 8 cm^{-1} could be achieved using a 100 μm entrance slit, and 100 μm core diameter collection fibers were selected. Multiple 100 μm core collection fibers were aligned to form a vertical line of fibers at the spectrograph. The vertical dimension of the CCD chip determines the number of fibers that can be imaged by the detector. The height of the CCD camera used in the Raman system was 6.7 mm and hence 50 collection fibers were used.

Once the fibers were selected, the common end of the probe was designed to minimize the background Raman signal that would be generated by the probe itself. Fluorescence and Raman scattering generated in the delivery fibers by the excitation light will be incident on the tissue; this unwanted signal can be diffusely reflected from the tissue surface and enter the collection fibers. Similarly, elastically scattered light as well as diffusely and specularly reflected excitation light from the tissue returned into the collection fibers can generate fluorescence and Raman scattering in these fibers that is detected along with the tissue signal of interest. Thus, in designing a fiber optic probe for cervical tissue measurements, our approach was to minimize both types of interfering fiber signal using a combination of longpass and bandpass filters. Figure 1 shows a diagram of a transverse section of the probe designed (not to scale) that incorporates separate optical fiber legs for delivery of excitation light and collection of Raman scattered light. To minimize the size of the probe, the smallest commercially available filters were used.

The excitation fiber was placed along the outer edge of the probe; the output of the excitation fiber was focused with a 3 mm diameter quartz lens and reflected by a gold wire polished at a 57° angle to yield a 900 μm excitation spot at the tissue surface. A 3 mm diameter round bandpass filter (Omega Optical, Brattleboro, VT) was placed after the lens to transmit the excitation light but block the fluorescence and Raman scattering generated in the excitation fiber at longer wavelengths.

To reduce generation of fluorescence and Raman scattering in the collection fibers, an 8 mm diameter round holographic notch filter (Kaiser Optical Systems, Ann Arbor, MI) that blocks the excitation light with an optical density (OD) of 6 and transmits at the longer wavelengths with an efficiency of 90%, was placed between the sample and collection fibers. The notch filter performance is optimal for collimated incident light, so scattered light from the tissue was collimated before the filter using a quartz lens and a second quartz lens refocused the light transmitted through the filter onto a group of 50 close-packed 100 μm core diameter optical fibers. The distal

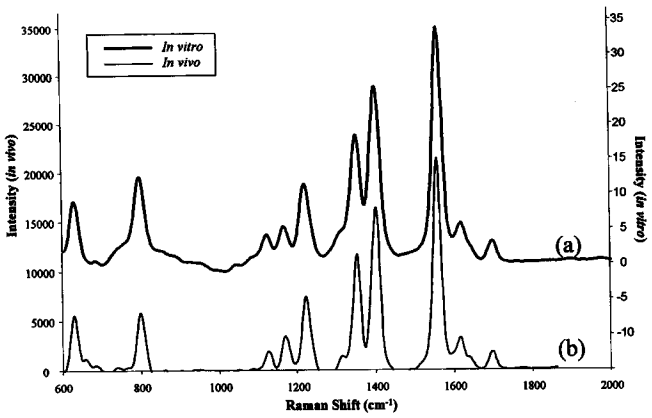

Figure 2. The NIR Raman spectra from rhodamine (a) measured with the *in vitro* system used in Mahadevan-Jansen *et al.* (9) and (b) measured with the *in vivo* system and probe shown in Fig. 1.

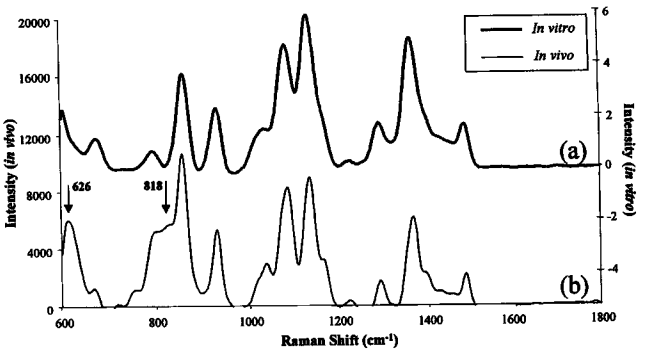

Figure 3. The NIR Raman spectra from a dilute solution of glucose (a) measured with the *in vitro* system used in Mahadevan-Jensen *et al.* (9) and (b) measured with the *in vivo* system and probe shown in Fig. 1.

ends of these fibers are arranged in a line and imaged onto the entrance slit of the spectrograph.

One of the collection fibers was directed to form an additional leg that was coupled to a 632.8 nm helium–neon laser, to provide an aiming beam for accurate probe placement on the sample. A quartz shield was used at the tip of the common end of the probe forming a barrier between the probe optics and the sample. The inner surfaces of the metal tubings used to house the probe optics were anodized black to reduce the incidence of multiple reflections of light.

All spectra measured with the system were corrected for the non-uniform spectral response of the entire system, including the fiber probe, the spectrograph and detector. Correction factors were generated by measuring the spectrum of a calibrated source.

The laser power at the tip of the probe was 15 mW with a spot size of 900 μm. The power of the excitation light source could potentially be increased to further improve the S/N and/or to reduce the integration time. However, the threshold limit value (TLV) established by the American Conference of Governmental Industrial Hygienists, Inc. (ACGIH) for skin exposure to 789 nm laser radiation without adverse health effects is 0.3 W/cm^2 (14). This corresponds to 1.9 mW of power for a 900 μm spot that is approximately eight times lower than that provided by our source. However, the 1996 ACGIH publication of TLV notes that these "values should be used as guides in the control of exposures and should not be regarded as fine lines between safe and dangerous levels" (14). Thus, supplementary methods of analysis were performed to investigate potential thermal effects of laser exposures in excess of the TLV.

Simulations were performed to calculate the expected rise in temperature due to laser radiation exceeding the TLV in Raman measurements of tissues. Light distribution was simulated using a Monte Carlo model for the specific illumination conditions of our probe using optical properties for cervical tissue (from unpublished data measured and calculated by the author). The expected temperature rise was then calculated using an implicit finite difference thermal model (15). The thermal model assumes no perfusion and an air medium surrounding the tissue during irradiation. The model does not take into consideration the cooling effects of perfusion and evaporation; this can result in an overestimation of the rise in temperature calculated by this model (16). For cervical tissue, given 15 mW of power incident on a spot diameter of 900 μm at 789 nm, the predicted temperature rise is only 1.5°C after 5 min. This temperature rise is well below that known to produce cytotoxicity (17); thus, we conclude this power level is reasonable for *in vivo* spectroscopy experiments.

System performance

Calibration standards. To validate system performance, the spectra of standards with known Raman signals, including rhodamine 6G, naphthalene and potassium iodide, were measured using the fiber optic Raman system. Background signal generated when no sample was present was also measured prior to each sample measurement. Finally, a weak solution of glucose was prepared such that its Raman intensity was similar to that of cervical tissue and the Raman spectrum was measured using the fiber optic system. All spectra were processed to remove background noise and fluorescence using a previously described method (10). Processed glucose spectra were compared with glucose spectra from published reports to ascertain that processing did not distort Raman spectra from weak samples.

Clinical measurements. A protocol to acquire *in vivo* Raman spectra was reviewed and approved by the Internal Review Boards of the University of Texas at Austin and the University of Texas MD Anderson Cancer Center. Patients at the colposcopy clinic of the MD Anderson Cancer Center with suspected cervical lesions were asked to participate in the *in vivo* Raman spectroscopy study. An informed consent was obtained from each participating patient. Raman spectra were acquired from about two sites in each patient after colposcopic examination of the cervix. An integration time of 90 s was used for each tissue spectral acquisition. Biopsies were obtained only from colposcopically abnormal sites analyzed by the probe and histology was performed.

RESULTS

The signal obtained with the probe in air showed Raman peaks associated with silica at 400, 626 and 818 cm^{-1} and no fluorescence generated by the probe materials is observed. Although the generation of silica signal by the excitation and collection fibers in the probe is minimized, the optical components in the probe are made of quartz yielding the observed remnant silica signal. Rhodamine spectra obtained with 20 s integration time are shown in Fig. 2. The two spectra were acquired using (a) the previously described *in vitro* system (10) and (b) the current *in vivo* system. The improved spectral resolution of the *in vivo* system from 11 cm^{-1} to 8 cm^{-1} results in better resolved peaks as can be seen in Fig. 2.

Because the Raman intensity of rhodamine is substantially greater than that of tissue, a dilute concentration of glucose was used as a weaker standard to verify that accurate spectra could also be obtained from samples with spectroscopic signals closer to that of tissue. Measured glucose spectra were compared with glucose spectra from published reports (18), as well as with spectra acquired using the *in vitro* system (10). Results are shown in Fig. 3, which shows that except for the interference of two silica peaks at 626 and 818 cm^{-1}, the Raman bands of glucose match those previously published (10,18).

Figure 4 shows the Raman spectra of a colposcopically

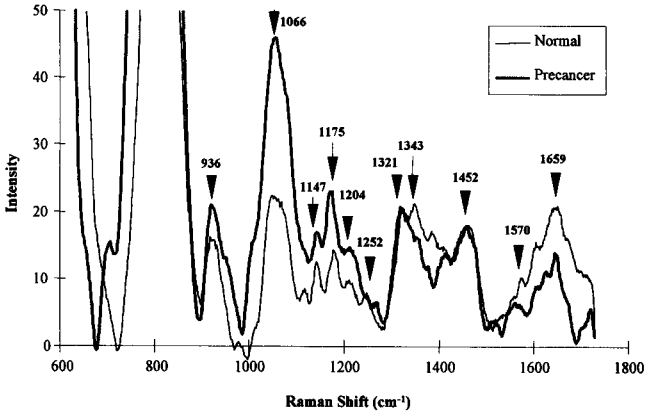

Figure 4. *In vivo* NIR Raman spectra from one normal and one abnormal site in a typical patient.

normal and precancerous site investigated in a typical patient. Silica peaks, observed at 626 and 818 cm^{-1} obscure any tissue peaks in this region. Examination of the spectra between 900 and 1800 cm^{-1} indicate that tissue peaks are observed at 936, 1066, 1147, 1175, 1204, 1252, 1321, 1343, 1452, 1570 and 1659 cm^{-1}. Previous *in vitro* work indicated that the ratios of unnormalized intensities at 1659 to 1321 cm^{-1} and at 1659 to 1452 cm^{-1} are useful in identifying cervical precancers (9,10). In the *in vivo* spectra shown in Fig. 4, the ratio at 1659 to 1321 cm^{-1} is 0.66 and the ratio at 1659 to 1452 cm^{-1} is 0.7 for the spectrum of colposcopically abnormal tissue. Based on these values, our previously developed algorithm would classify the colposcopically abnormal sample as a high grade precancer. The histology for this patient indicated that the colposcopically abnormal site did contain high grade precancer; this lesion was incorrectly identified as a human papilloma viral infection under colposcopic impression by the participating practitioner. The ratio at 1659 to 1321 cm^{-1} is 1.01 and the ratio at 1659 to 1452 cm^{-1} is 1.16 for the spectrum of colposcopically normal tissue. Thus our algorithm also classifies the colposcopically normal sample as a high grade precancer. However, since histology was not performed on the normal samples this diagnosis could not be confirmed.

DISCUSSION

These results indicate that *in vivo* Raman spectra have the potential to provide the diagnostic information necessary to distinguish between precancers and nonprecancers. However, *in vivo* Raman spectra from more patients need to be analyzed to assess the diagnostic capability of *in vivo* Raman spectroscopy. *In vivo* Raman spectra observed here appear similar to *in vitro* Raman spectra obtained from cervical biopsies above 900 cm^{-1} (9,10). Comparison of the Raman peaks observed in cervical tissue spectra acquired *in vivo* and *in vitro* show similar primary Raman peaks with three major exceptions. A Raman band at 936 cm^{-1} is observed *in vivo* but not *in vitro*. *In vitro* Raman spectra showed a peak at 978 cm^{-1} that is not consistently observed *in vivo*. The amide band at 1252 cm^{-1} is not as prominent *in vivo* as *in vitro*. All other Raman peaks appear similar *in vivo* as well as *in vitro*.

Spectra acquired using the described Raman probe were found to be in general superior (better S/N and more sensitive) to most commercially available probes due to the large number of collection fibers, accurate filters and specific design of the probe (unpublished data). *In vivo* Raman spectra measured here still display an overlap of silica and tissue Raman signal, indicated by the intense Raman peaks at 626 and 818 cm^{-1}. It is hypothesized that although some contribution to this interfering signal may arise from the fibers and optics used in the probe, the primary source of this signal is the quartz shield used as a barrier between the probe and the sample. A thinner quartz shield may reduce this background signal but will not eliminate it. Other materials that could potentially be used as a window are sapphire and transparent Teflon. These materials have a distinct but narrow Raman band(s) that would be detected by the probe but that may be eliminated easily. A probe with a removable window would allow several different materials to be tested before making an appropriate selection.

Another possible improvement to the clinical Raman system is the use of a higher power laser source. Given the spot size at the sample from the Raman probe, Monte Carlo and thermal modeling predict that a laser power of up to 80 mW could be used with a corresponding rise in cervical tissue temperature of 6°C/min. A stronger laser in conjunction with the remaining modifications made to the clinical system could potentially reduce the integration time to 15–20 s.

Acknowledgements—The authors thank Dr. E. Duco Jansen for his collaboration with Monte Carlo simulations and thermal modeling and Douglas Heintzelman for his help in spectral calibration of the system.

REFERENCES

1. Frank, C. J., R. L. McCreery, and D. C. Redd (1995) Raman spectroscopy of normal and diseased human breast tissues. *Anal. Chem.* **67**, 777–783.
2. Manoharan, R., K. Shafer, L. Perelman, J. Wu, K. Chen, G. Deinum, M. Fitzmaurice, J. Myles, J. Crowe, R. R. Dasari, and M. S. Feld (1998) Raman spectroscopy and fluorescence photon migration for breast cancer diagnosis and imaging. *Photochem. Photobiol.* **67**, 15–22.
3. Berger, A. J., I. Itzkan, and M. S. Feld (1995) Noninvasive concentration measurements of dissolved analytes in human whole blood by Raman spectroscopy. *Photochem. Photobiol.* Suppl. **61**.
4. Puppels, G. J., T. C. Bakker Schut, R. Wolthius, P. J. Caspers, and H. A. Bruining (1998) In vitro and in vivo tissue characterization by Raman spectroscopy. In *Infrared Spectroscopy: New Tool in Medicine.* Vol. 3257 Edited by H. H Mantsch and M. Jackson). *SPIE,* Bellingham, WA.
5. Schrader, B., S. Keller, T. Loechte, S. Fendel, D. S. Moore, A. Simon and J. Sawatzki (1995) NIR FT Raman spectroscopy in medical diagnosis. *J. Mol. Struct.* **348**, 293–296.
6. Lawson, E. E., B. W. Barry, A. C. Williams, and H. G. M. Edwards (1997) Biomedical applications of Raman spectroscopy. *J. Raman Spectrosc.* **28**, 111–117.
7. Liu, C. H., B. B. Das, W. L. Sha Glassman, G. C. Tang, K. M. Yoo, H. R. Zhu, D. L. Akins, S. S. Lubicz, J. Cleary, R. Prudente, E. Celmer, A. Caron, and R. R. Alfano (1992) Raman, fluorescence and time-resolved light scattering as optical diagnostic techniques to separate diseased and normal biomedical media. *J. Photochem. Photobiol. B Biol.* **16**, 187–209.
8. Feld, M. S., R. Manoharan, J. Salenius, J. Orenstein-Carndona, T. J. Romer, J. F. Brennan III, R. R. Dasari, and Y. Wang (1995) Detection and characterization of human tissue lesions with near infrared Raman spectroscopy. In *Advances in Fluorescence Sensing Technology II,* Vol. 2388 (Edited by J. R. Lakowicz), pp. 99–104. *SPIE,* Bellingham, WA.

9. Mahadevan-Jansen, A., R. Richards-Kortum (1996) Raman spectroscopy for the detection of cancers and precancers. *J. Biomed. Optics* **1**, 31–70.
10. Mahadevan-Jansen, A., M. F. Mitchell, N. Ramanujam, A. Malpica, S. Thomsen, U. Utzinger and R. Richards-Kortum (1998) Near-infrared Raman spectroscopy for the diagnosis of cervical precancers. *Photochem. Photobiol.* **68**. (In press)
11. Myrick, M. L., S. M. Angel and R. Desiderio (1990) Comparison of some fiber optic configurations for measurement of luminescence and Raman scattering. *Appl. Optics* **29**, 1333–1344.
12. Shim, M. G. and B. C. Wilson (1997) Development of an in vivo Raman spectroscopic system for diagnostic applications. *J. Raman Spectrosc.* **28**, 131–142.
13. Mahadevan, A. (1996) Fluorescence and Raman spectroscopy for diagnosis of cervical precancers, Ph.D. Dissertation, The University of Texas at Austin.
14. ACGIH (1996) Threshold limit values for chemical substances and physical agents, biological exposure indices. *American Conference of Governmental Industrial Hygienists,* Cincinnati, OH.
15. Incropera, F. P. and D. P. De Witt (1990) *Fundamentals of Heat and Mass Transfer,* John Wiley & Sons, New York.
16. Torres, J. H., M. Motamedi, J. A. Pearce and A. J. Welch (1993) Experimental evaluation of mathematical models for predicting the thermal response of tissue to laser irradiation. *Appl. Optics* **32**, 597–606.
17. Thomsen, S. (1991) Pathologic analysis of photothermal and photomechanical effects of laser–tissue interactions, *Photochem. Photobiol.* **53**, 825–835.
18. Goral, J. and V. Zichy (1990) Fourier transform Raman studies of materials and compounds of biological importance, *Spectrochim. Acta* **46A**, 253–275.